Transactions, SMiRT-24
BEXCO, Busan, Korea - August 20-25, 2017
Division IX (include assigned division number from I to X)

EFFECT OF WELDING RESIDUAL STRESS ON THE CREEP BUCKLING BEHAVIOR OF FAST BREEDER REACTOR

Fang Liu[1], Jian-Guo Gong[2], Fu-Zhen Xuan[3]

[1] PhD Student, East China University of Science and Technology, China
[2] Lecturer, East China University of Science and Technology, China
[3] Professor, East China University of Science and Technology, China

ABSTRACT

Creep buckling is a common failure mode for some structures in Fast Breeder Reactor (FBR), such as support cylinder, and so on. The effect of welding residual stress on the creep buckling behavior of support cylinder under axial compressive load was simulated using the shell-to-solid coupling method, where the welding joint and its adjacent zone were built utilizing solid submodel and the zone far away from the welding joint was modeled by shell submodel. Three analyses were established: a thermal analysis, a residual stress analysis and a creep buckling analysis. Results indicate that creep buckling time of the support cylinder is prolonged due to the welding residual stress under load levels mentioned, implying that the current design method causes a conservative result without considering the welding residual stress.

INTRODUCTION

It is well known that FBR are operating at high temperatures and creep is an important issue that should be taken into account. For some thin-walled structures in FBR, buckling may interact with creep. For example, in Chinese experiment fast reactor (Cui et al. 2013), the equipments (i.e., intermediate heat exchanger, air heat exchanger and pump) are supported by cyliderical shell and large weights are concentrated on the top of these support cylinders, so creep buckling is a common failure mode for these support cylinders. Design codes, such as ASME-NH (2015) and RCC-MR (2007) use design factor rules to guard against creep buckling only with the geometrical imperfection and tolerances into consideration. For practical engineering structures, however, the welding residual stress is an unavoidable factor, but neither of these codes have taken welding residual stress into consideration. Therefore, it is necessary to study the effect of welding residual stress on the creep buckling behavior of FBR.

In the past decades, the creep buckling behavior has been reported by many researchers. Morovat et al. (2014) studied the creep buckling behavior of steel columns subjected to fire. In his work, the analytical and computational predictions of creep buckling behaviour were developed. It was concluded that neglecting creep effects can lead to erroneous and unsafe predictions of the strength of steel columns subjected to fire. Korobeynikov et al. (2013) conducted a simulation of creep buckling in terms of axially compressed circular cylindrical shells using the MSC.Marc 2012 software. It was found that for large axial compressive stresses, the buckling modes under creep condition predicted by theoretical and experimental were in satisfactory agreement. In addition, a review paper for creep buckling was reported by Turbat and Drubay (2002).

As far as the authors know, limited papers are reported about the effect of the welding residual stress on creep buckling behavior, but the welding residual stress is included when analyzing the buckling strength of shell structure. For example, Gong et al. (2017) investigated the residual stress and its effect on the buckling behavior of storage tanks subjected to harmonic settlement, with user subroutine method employed when studying the residual stress. It was concluded that the welding residual stress has a strengthening effect on the buckling behavior. Hübner et al. (2006) reported the buckling behavior of

large scale steel cylinders with pattern welds, where the welding residual stress was simulated using the shrinkage strain approach. Similar conclusion was also obtained about the effect of the residual stress. Although these papers have reported that the residual stress has positive effect on buckling behavior, more works is needed to confirm it still hold for creep buckling behavior.

Regarding the analysis of the welding residual stress, many methods have been adopted, such as the temperature history method, shrinkage strain approach, user subroutine method (ABAQUS), and so on. Among all these methods, the user subroutine method in ABAQUS is widely adopted for describing the welding residual stress of many engineering structures (Liu et al. 2011; Deng et al. 2009) and it is usually realized by an indirect coupling analysis: The first step is to calculate a temperature field analysis of the welding process using the user subroutine DFLUX; the second step is to conduct a stress field analysis through importing the result file of the thermal analysis of the first step. This analysis procedure will be employed in this work.

In general, the 3D shell model is adequate and accurate to study the creep buckling behavior of shell structure under axial compressed stress, but it cannot describe the welding residual stress across the thickness section. To settle this problem, the shell-to-solid coupling method (Dassault 2011) is adopted, which allows for a transition from shell element modeling to solid element modeling. The analysis procedure is usually as follows: First, the weld part and its adjacent zone are built using the 3D solid submodel, and the zone away from the weld is established using the shell submodel. Then, the shell and the solid are joined together by shell-to-solid coupling method.

NUMBERICAL MODEL

Geometrical Model and Analysis Strategy

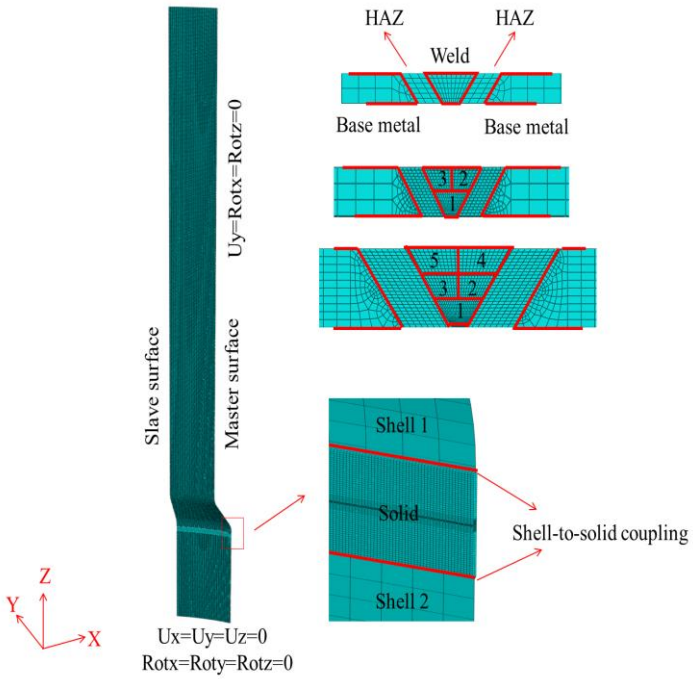

Figure 1. Model of support cylinder

The model adopted in this work is a variable diameter support cylinder and the thickness is 5mm. In order to investigate the effect of thickness on creep buckling behavior, another two models are found with the thicknesses as t=3mm and 10mm. A three-dimentional finite-element model using the finite-

element computer package ABAQUS is established. Taking the symmetry of the model into consideration, the sixteenth model is employed. The welding joint and its adjacent zone are built using the 3D solid submodel, while the shell away from the welding joint is established using the shell submodel. Then, the shell model and the solid model are coupled together using the shell-to-solid coupling method. The welding joint studied is located between the lower cylinder and straight segment.

Three analyses should be established: First, carry out a thermal analysis to describe the temperature field during the welding process. Then, conduct a stress analysis of the welding process through importing the thermal results of the first step. Finally, develop a creep buckling analysis by restart analysis with the welding residual stress generated in the second analysis. Through the above analyses, the effect of the welding residual stress on the creep buckling behavior of support cylinder can be investigated.

Mesh Model and Material Properties

As previously described, the solid and shell submodel is used in this work. For the first analysis, the solid part is discretized using the eight-node and hexahedral solid element (DC3D8), while the shell part is meshed by the four-node and quadrilateral shell element (DS4). For the other analysis, the solid part is discretized using the eight-node and hexahedral solid element (C3D8), while the shell part is meshed by the four-node, quadrilateral, and reduced integrated shell element (S4R). The mesh models of the welding joint for different thicknesses are shown in Figure 1. Multipass welding is adopted for t=5mm and 10mm.

For the material properties, the whole finite-element model is assumed to have the same material properties as SS316L, and temperature-dependent material properties are adopted for simulations. The detailed mechanical and physical parameters are based on the data from Dong (2001), shown in Figure 2. It should be noted that for material properties at the temperature higher than1460℃, it is assumed that they are the same as that of the temperature of 1460℃. Besides, different operating temperatures are considered and Norton-Bailey creep model is adopted for creep analysis. The strain-hardening form of this model is shown as equation (1), and the detail parameters at different temperatures are from Mathew et al. (2015) shown in Table 1.

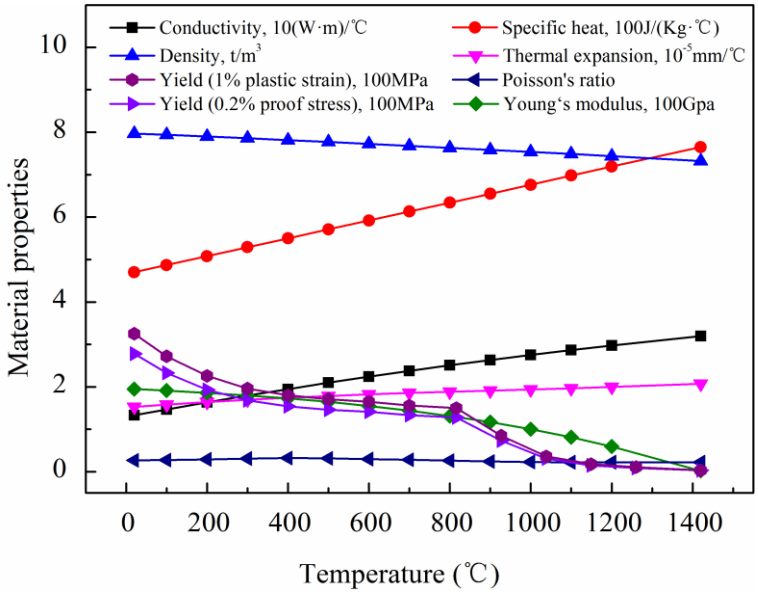

Figure 2. Material parameters of SS316L at various temperatures

Table 1. Parameters for Norton-Bailey creep model

Temperature/℃	A	n
550	4.79×10^{-31}	8.74
600	1.95×10^{-24}	6.08
650	1.13×10^{-20}	8.30

$$\dot{\varepsilon}_c = A\sigma^n \tag{1}$$

where $\dot{\varepsilon}_c$ is creep strain rate; σ is stress; A and n are material constants.

Main Boundary Conditions

Main boundary conditions of the three analyses are listed below: (1) For the first analysis (thermal analysis), the heat flux is imposed to the elements of welding passes by a user subroutine DFLUX. Meanwhile, the convection coefficient and the initial temperature are set as 10 W/(m^2℃) and 20℃, respectively. (2) For the second analysis (welding residual stress), cyclic symmetry are adopted and symmetrical constraints are imposed at the master surface with the normal direction of Y-axis (see Figure 1). All freedoms of upper and lower boundary are constrained. Meanwhile, the thermal results are imported for residual stress analyses. (3) For the third analysis (creep buckling analysis), the boundary conditions are nearly the same as that for the stress analysis expect that at the upper cutting plane, where no axial loading is applied.

Thermal Analysis of Welding

The welding process is modeled by a user subroutine DFLUX in ABAQUS for each welding pass and a double ellipsoidal distribution (Goldak et al. 1984) is employed for thermal analysis. The front q_f and rear q_r power density in two ellipsoidal quadrants are formulated by the equations (2)-(3):

$$q_f = \frac{6\sqrt{2}\eta UI}{\pi\sqrt{\pi}a_o b_o c_o}\exp\left[-3\left(\frac{x_g^2}{a^2}-\frac{y_g^2}{b^2}-\frac{z_g^2}{c_f^2}\right)\right] \tag{2}$$

$$q_r = \frac{6\sqrt{2}\eta UI}{\pi\sqrt{\pi}a_o b_o c_o}\exp\left[-3\left(\frac{x_g^2}{a^2}-\frac{y_g^2}{b^2}-\frac{z_g^2}{c_r^2}\right)\right] \tag{3}$$

where η represents the efficiency factor; U is the arc voltage; I is the welding current; x_g, y_g and z_g are relative distances from the arbitrary point (x, y, z) to the moving coordinate system; a, b and c are the width, depth and length of the heat source, respectively; c_f and c_r represent the value for front and rear parts in the model.

The *MODEL CHANGE option in ABAQUS (element birthand death technology) is adopted to add and remove the elements in welding passes.

Welding Residual Stress Analysis

When the thermal analysis of the welding process is completed, the welding residual stress can be analyzed. As previously mentioned, the shell-to-solid coupling technology is adopted for analyses, so the

*SHELL TO SOLID COUPLING option in ABAQUS is employed. As shown in Figure 1, two coupling regions are established. Similar to the thermal analysis of the welding process, the *MODEL CHANGE option in ABAQUS is adopted to add and remove the elements in welding passes. Considering that the restart analysis is necessary in following creep buckling analysis, *EDIT RESTART REQUESTS option is employed. It should be noted that the steps built are the same as that for the thermal analysis and the thermal results need to be imported.

Creep Buckling Analysis

In order to simulate creep buckling behavior, a restart analysis is employed and a visco step should be added following the welding residual stress analysis. Then axial compressed load which is a fraction of the zero-time buckling load is applied on the upper boundary, and gravity is also exerted. The Norton-Bailey law is adopted for the creep analysis studied. It should be pointed out here that to get the zero-time buckling load, an inelastic load-deflection analysis has to be performed. This has been done by adding a riks step following the welding residual stress analysis.

RESULTS AND DISCUSSIONS

Distribution of Welding Residual Stress

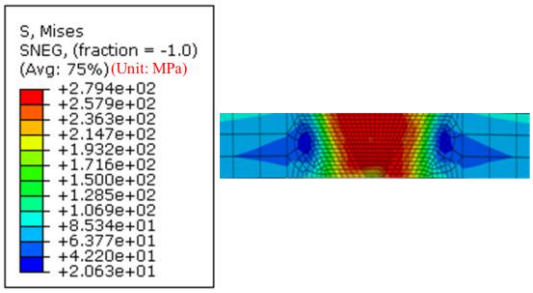

(a) Mises stress

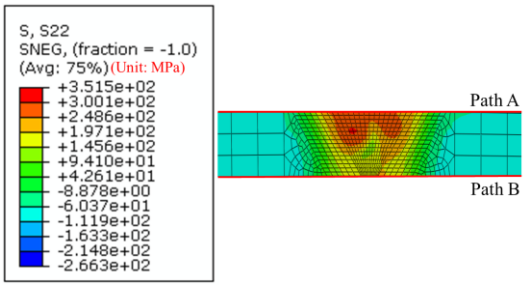

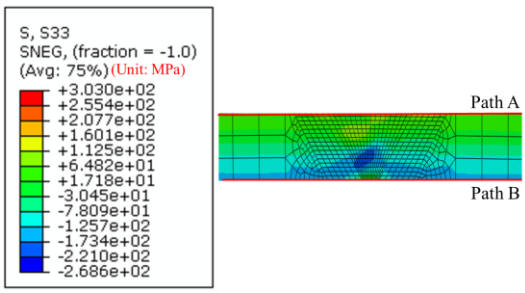

(b) Hoop stress (c) Axial stress

Figure 3. Distribution of welding residual stress (t=5mm)

The distributions of welding residual stress for t=5mm are shown in Figure 3. It can be found that the maximum value of the hoop and axial welding residual stress are both located at the third welding pass close to outer wall surface. Meanwhile, the residual stress in the hoop direction is higher than that in the axial direction.

Paths A and B (see Figure 3(b) and 3(c)) are chosen to describe the hoop and the axial welding residual stress distributions of the welding joint, displayed in Figure 4. The vertical axis is the axial/hoop stress and the horizontal axis represents the distance from a point of paths A and B to the center of the

welding zone. It should be noted that the paths A and B are along the outer and inner wall surfaces, respectively. It can be observed that for the hoop stress, the stress values at the welding zone of both paths are much higher than that at the fusion and the HAZs, and it drops significantly for the zone away from the welding joint. Meanwhile, the maximum hoop stress of the welding zone for path A is higher than that for path B. For the axial stress, the compressive axial stress is observed for path A in the welding zone, while the axial stress for path B in the welding zone is in the tensile state. The similar results can be found for another two cases with thickness of t=3mm and 10mm.

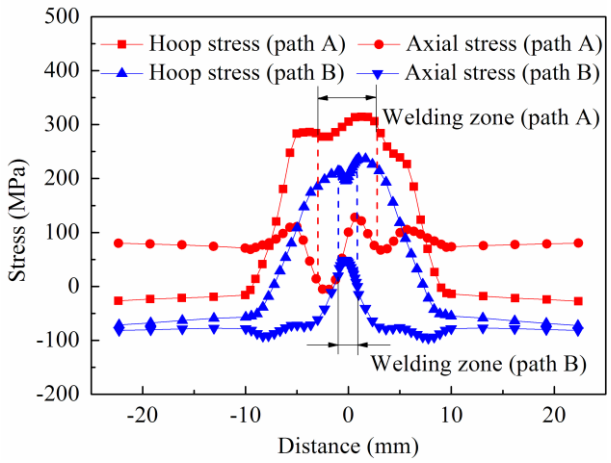

Figure 4. Welding residual stress distributions along paths A and B (t=5mm)

Effect of Welding Residual Stress on Creep Buckling Time

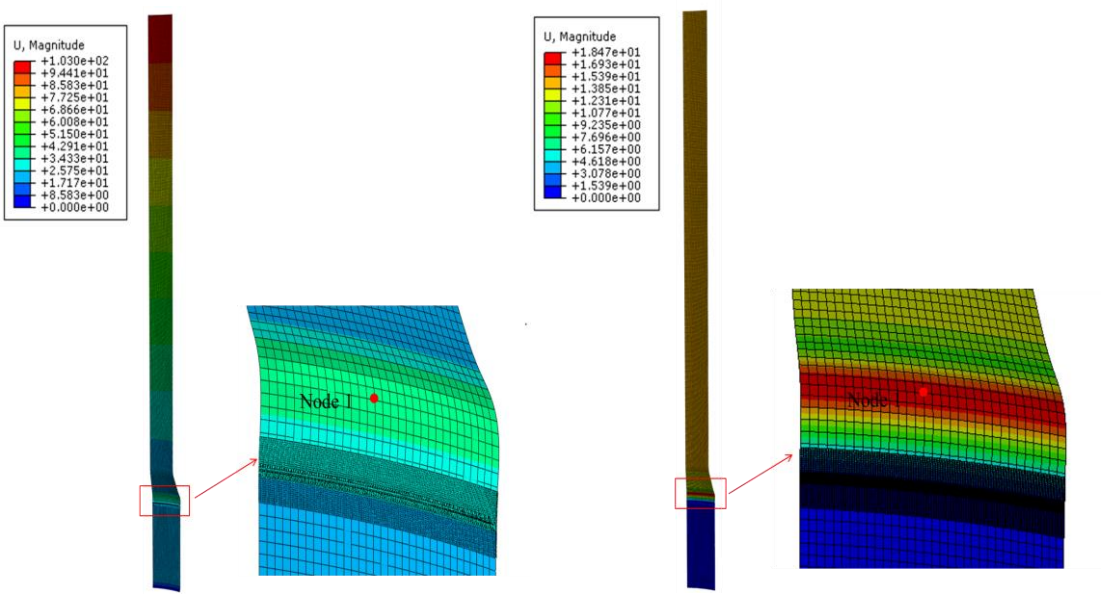

(a) With residual stress (n=1.65) (b) Without residual stress (n=1.65)

Figure 5. Creep buckling modes of support cylinder (t=5mm, T=600℃)

The creep buckling modes of the support cylinder subjected to axial compressive load at 600℃ for t=5mm are presented in Figure 5. It is indicated that when the welding residual stress is taken into

consideration, the buckling distortion mainly occurs at the upper boundary, while the buckling distortion takes place at the lower fillet without the the welding residual stress. Meanwhile, the magnitude of the shell displacement presents a siginificant difference. The reason for the difference is mainly due to the welding deflection.

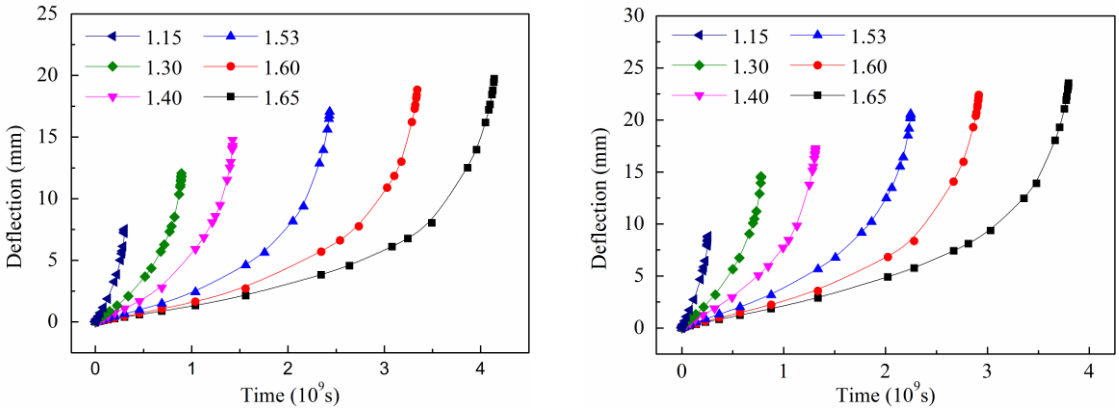

(a) With residual stress (b) Without residual stress

Figure 6. Deflection due to creep (t=5mm, T=600℃)

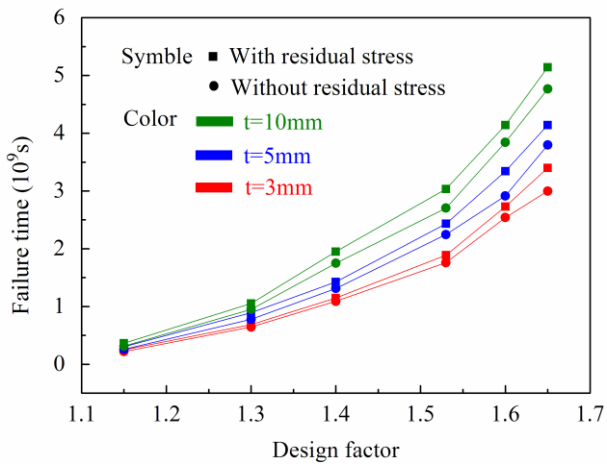

Figure 7. Creep buckling curves (T=600℃)

The results of creep buckling are presented in Figure 6 as plots of deflection at node 1 (critical node) versus time at various design factors n (n=applied compressed load/zero-time buckling load). It clearly shows that the rate of change of displacement with time increases very slowly at the beginning and then increases more rapidly until the endurance limit of the structure. The time at which the displacement-time curves become nearly vertical is taken as the failure time in this study.

It can be found from Figure 7 that the introduction of welding residual stress can prolong the creep buckling time for all cases stufied. Meanwhile, similar conclusion can be found at T=550℃ and 650℃. The reason for the strengthening effect of welding residual stress on creep buckling time is the decrease of the stress with the the residual stress included. .

As shown in Figure 8, the vertical axis is the Mises/hoop/axial stress at node 1 and the horizontal axis represents time. The same tendency can be found in Figure 8(a)(b)(c). When taking the residual stress and welding deformation into consideration, the magnitude of stress goes straight down from the residual tensile stress, then it increases very slowly at the beginning and increases more rapidly until the

failure of the structure. For the situation without residual stress, tensial stress is observed under compressed load, then it is higher than that with residual stress during the whole life. Actually, the welding residual deformation has a remarkable effect on the stress state under axial compressed load. During the welding process, outward deformation at welding joint results from welding tensile stress. When the creep buckling analysis is implemented by restart analysis, structure characteristics change due to the welding residual deformation, so that the compressed stress instead of tensile stress occurs and the magnitude of stress at node1 goes straight down from the residual tensile stress.

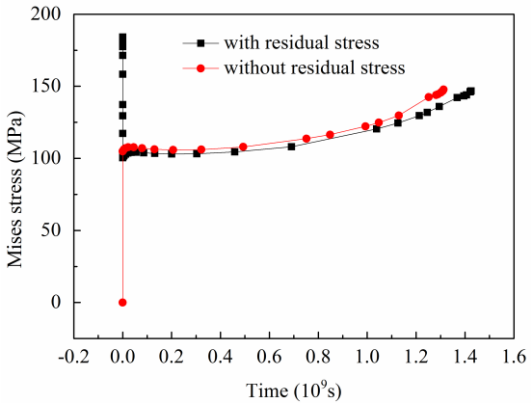

(a) Mises stress at node 1

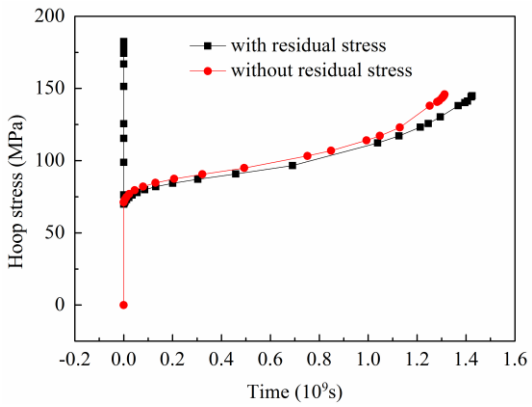

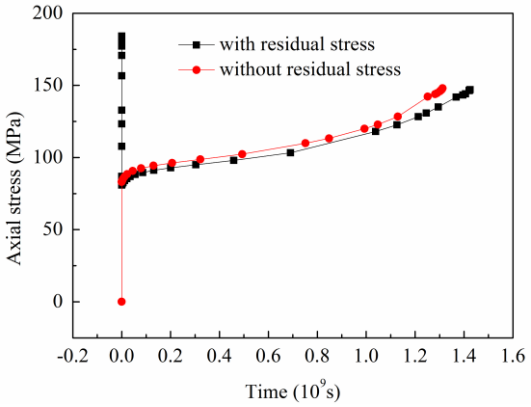

(b) Hoop stress at node 1 (c) Axial stress at node 1

Figure 8. Creep buckling curves (T=600℃)

CONCLUSIONS

The effect of the welding residual stress on creep buckling behavior of the support cylinder under compressed load was investigated through numerical analyses, using the shell-to-solid coupling method. Results show a strengthening effect of residual stress on creep buckling time of support cylinder under axial compressed load. Meanwhile, the buckling modes of support cylinders is different due to the welding deformation. In addition, to reduce the conservation of support cylinder design, the welding residual stress should be taken into consideration when conducting a structural design of the support cylinder under axial compressed load.

REFERENCES

ASME Boiler & PressureVessel Committee (2015). *ASME Boiler and Pressure Vessel Code Section III, Subsection NH*, ASME.

Cui, M., Guo, Y., and Zhang, Z. (2013). "Transient simulation code development of primary coolant system of chinese experimental fast reactor," *Annals of Nuclear Energy*, 53, 158-169.

Dassault (2011). "Abaqus 6.11 User's Manual," Dassault Systems SIMULIA, Providence, RI.

Deng, D. (2009). "FEM prediction of welding residual stress and distortion in carbon steel considering phase transformation effects," *Materials & Design*, 30(2), 359-366.

Dong, P. (2001). "Residual stress analyses of a multi-pass girth weld: 3-d special shell versus axisymmetric models," *Journal of Pressure Vessel Technology*, 123(2), 207-213.

Goldak J, Chakravarti A and Bibby M (1984). "A new finite element model for welding heat sources," *Metallurgical and Materials Transactions B*, 15(2): 299-305.

Gong J G, Yu L, Wang F, et al (2017). "Effect of Welding Residual Stress on the Buckling Behavior of Storage Tanks Subjected to Harmonic Settlement," *Journal of Pressure Vessel Technology*, 139(1): 011401.

Hübner, A., Teng, J. G., and Saal, H. (2006). "Buckling behaviour of large steel cylinders with patterned welds," *International Journal of Pressure Vessels & Piping*, 83(1), 13-26.

Korobeynikov, S. N., Torshenov, N. G., Lyubashevskaya, I. V., Larichkin, A. Y., and Chunikhina, E. V. (2013). "Creep buckling of axially compressed circular cylindrical shells of a zirconium alloy: experiment and computer simulation," *Journal of Applied Mechanics & Technical Physics*, 55(1), 105-117.

Liu, C., Zhang, J. X., and Xue, C. B. (2011). "Numerical investigation on residual stress distribution and evolution during multipass narrow gap welding of thick-walled stainless steel pipes," *Fusion Engineering & Design*, 86(4–5), 288-295.

Mathew, M. D., Ganesan, V., Ganesh Kumar, J., and Laha, K. (2015). "Creep properties and design curves for nitrogen enhanced grade of 316LN stainless steel," *Materials at High Temperatures*, 32(4), 363-368.

Morovat, M., Engelhardt, M., Helwig, T., and Taleff, E. (2014). "High-temperature creep buckling phenomenon of steel columns subjected to fire," *Journal of Structural Fire Engineering*, 5(3), 189-202.

RCC-MR (2007). *Design and Construction Rules for Mechanical Components of FBR Nuclear Islands*, Paris, AFCEN.

Turbat, A., and Drubay, B. (2002). "Buckling Analysis in Creep Conditions: Review and Comparison," *10th International Conference on Nuclear Engineering*, American Society of Mechanical Engineers, 741-746.